

STRATIFIED FLUID EXPERIMENTS IN AN ANNULUS WITH SLOPING INNER WALL UNDER SLIGHT MODULATION OF THE ROTATION SPEED

Leo Maas, Uwe Harlander, Astrid Manders (Physical Oceanography, Royal Netherlands Institute for Sea Research (NIOZ) , PO Box 59, 1790 AB Den Burg, the Netherlands) and Arno Swart (Computational Sciences, University of Utrecht)

Abstract

Experiments have been performed in Coriolis Laboratory, Grenoble, in a continuously-stratified rotating fluid, contained in an annular shaped region having a sloping inner wall. Waves were forced by weak modulation of the rotation speed. This results in an oscillatory Ekman transport over the slope. During the downwelling phase this has led to static instabilities and mixing. Convergence of Ekman transport also drives internal waves, that are subject to geometric focusing and again mixing over some range of forcing periods. Both mechanisms thus appear to contribute to massive mixing (and subsequent mean flow and Rossby wave generation). With an additional radial barrier inserted, the modulation mechanism more easily led to waves that propagate away from the barrier, albeit in a non-symmetric way. This suggests that refractive trapping of the wave depends on the background rotationsense.

1.1 Introduction

We will describe experiments that were carried out in a uniformly-stratified fluid, contained in an annulus having a sloping inner wall. The basin is rotating with a rotation speed Ω that has a weak modulation superimposed on it (providing the forcing). Two types of experiments were carried out: first, axisymmetric, and second, non-axisymmetric, in which a radial barrier is inserted.

The uniform stratification is characterized by a buoyancy frequency N taken equal to $N=4\Omega=2f$, where f is the inertial frequency. For modulation frequencies ω in the range $f<\omega<N$ internal waves of that frequency might arise. In the axisymmetric setting these may be excited by convergence of Ekman transport in the boundary layer over the slope or flat bottom. This is similar to the generation of inertial waves in axisymmetric experiments in homogeneous fluids by Beardsley (1970). When a radial barrier (extending to half the fluid depth) is inserted there is also a direct (inviscid) generation of internal waves, akin to the internal tide generation by cross-isobath tidal flow in a stratified sea.

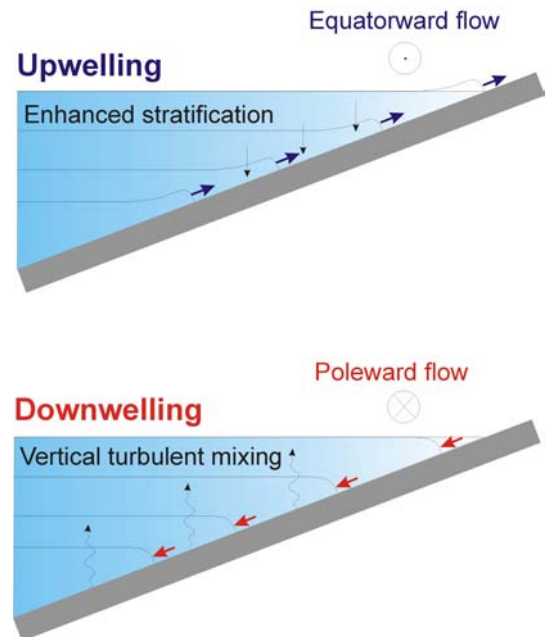


Figure 1: Assume we have a bottom sloping towards the east in the Northern Hemisphere. During two phases of an along-slope, oscillatory current (into and out of the paper) there is an upwelling and downwelling favorable Ekman flow in the bottom boundary layer. The latter might give rise to an instability.

There are two issues which the axisymmetric experiments in an annulus having a sloping wall might clarify. The first is that of the possibility of mixing due to an instability of the time-dependent Ekman layer below a modulating along-slope current (figure 1), see Trowbridge and Lentz (1991). The second is that internal waves that are generated in the manner described above may be subject to geometric focusing when the modulation frequency is chosen appropriately. Focusing of internal wave energy onto internal wave attractors may then lead to mixing at the slope, at the location where the focusing takes place, i.e. where the attractor reflects from the slope (figure 4), see Maas and Lam (1995). No matter which of the two occurs, any mixing will lead to a restratification entailing in a rotating system the generation of a geostrophic current. This may become baroclinically unstable, yielding finally low-frequency, baroclinic topographic Rossby waves.

The barrier in the non-axisymmetric experiments provides a clear additional, and presumably more powerful internal wave source. Internal waves may either be refractively trapped (onto an internal wave attractor in some specific radial plane, at a particular distance from the barrier), or they may propagate all along the annulus when refraction towards a local radial plane, is offset by subsequent refraction away from such a plane. The former case will be erroneously interpreted as one of strong damping. The present experiments aim at establishing their relative importance and the possibly asymmetric nature of the response (e.g. a difference between up and down-rotation penetration depth), due to background rotation.

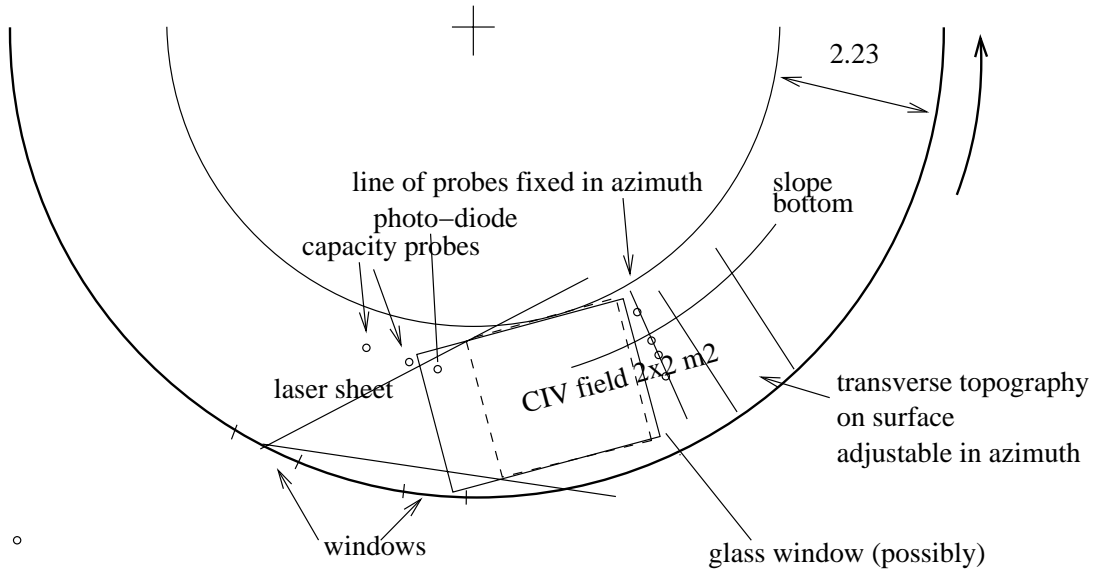


Figure 2: Schematic of 6.5m radius Coriolis tank. Annulus of 2.23m is at outer rim. Inner part of annulus consists of slope. Radial barrier inserted in second set of experiments.

1.2 Experiments

The experiments were carried out on the 13 m diameter Coriolis platform, Grenoble, in a fluid that is linearly stratified initially ($N=2f$), in an annular shaped tank. The annulus has a vertical outer wall at radius $R=6.5$ m, and an inner slope whose shape is a quarter sinusoid, starting flat at 1.45 m from the outer wall, and eventually rising linearly to the surface at 2.24 m from the outer wall (radius 4.26m). Fluid depth is 60 cm (neglecting the parabolic free surface distortion due to rotation). The tank is rotating during the whole experiment at an average rotation period $T=50$ s ($\Omega=2\pi/T$). Forcing was by modulation of the rotation speed, $\Omega[1+\varepsilon \sin(\omega t)]$ (with $\varepsilon=O(0.1)$), over some period of time τ .

vertical cut, scale 1/20

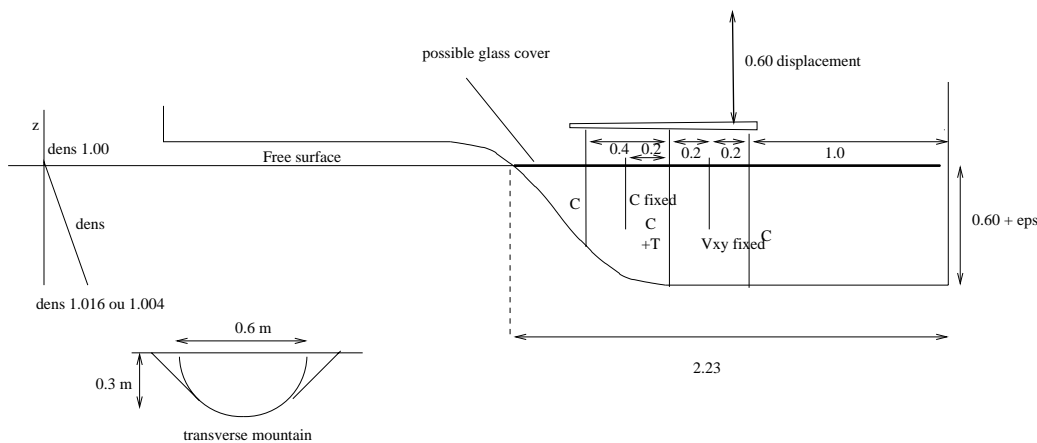


Figure 3: Schematic of cross-section of rotating annulus and of density profile. Actual instruments used are shown in figure 5. Also (at bottom) an inverted cross-section of the barrier that has been put radially on the bottom. The barrier extends to half the fluid depth.

The modulation is specified by (1) the modulation period ($T'=2\pi/\omega$) and (2) the speed at the rim (6.5 m radius) relative to the state of solid-body rotation ($V=\varepsilon\Omega R=6$ cm/s, hence $\varepsilon=V/\Omega R=0.0735$).

Three modulation periods T' have been used: (1) 22.53 s, (2) 19 s and (3) 21 s. The former two correspond to a frequency for which a simply-shaped attractor is expected to arise in the radial direction (having either one or two reflections at surface and bottom, for the first two periods respectively, and just one reflection at the side and sloping walls – see e.g. fig. 4). These attractors arise because the internal waves propagate their energy obliquely, along a certain direction θ with the vertical, given by the dispersion relation

$$\omega^2 = N^2 \cos^2 \theta + f^2 \sin^2 \theta$$

The attractors present the only strictly periodic orbits, to which all ‘webs’ (rays, together with their reflections) tend. The third frequency is an ‘anti’ frequency, for which the theoretical shape of the attractor has many reflections at the walls and is therefore, in the presence of viscous effects, not likely to arise.

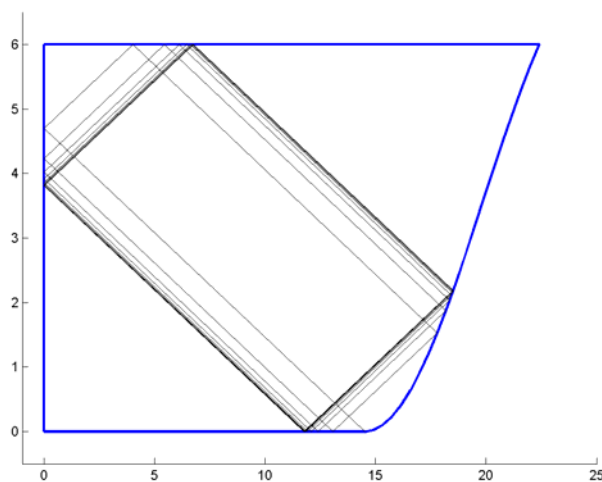


Figure 4 Cross-section with ray pattern of radially and vertically propagating internal waves of period $T'=22.53$ s, corresponding to a 1-1 attractor (solid rectangle).

In a second set of experiments a radial barrier extending 30 cm, i.e. half the fluid depth, was inserted. The shape of the barrier was nearly parabolic and had a base width of 80 cm.

Observations were performed by means of particle image velocimetry (PIV) with Coriolis' CIV-package. By changing the height of the laser sheet, velocity measurements were obtained at multiple levels (1,5 or 10). By changing the orientation of the laser sheet, also velocities in a vertical-radial plane were obtained (albeit not entirely covering the section). Simultaneously, observations were also made by means of contact sensors that measure

velocity, or density (of both ultrasonic as well as conductivity type). These probes were mounted on a carriage (motor) that either made vertical profiles (taking about 50 seconds for an up and downcast), or made time series at a height of 2 cm above the bottom. Some of the time series were interrupted every 5 minutes, to make such vertical profiles. The hybrid time series was disentangled by using a Matlab-program by F. Eijgenraam. We have used the following conductivity probes from which, through calibration, density profiles were obtained: ultrasonic probe, U5, at $r=6.08\text{m}$; conductivity probes, C1 at $r=5.50\text{m}$ and C2, at $r=5.10\text{m}$, and ultrasonic probes U1, at $r=4.90\text{m}$ and U2 at $r=4.70\text{m}$.

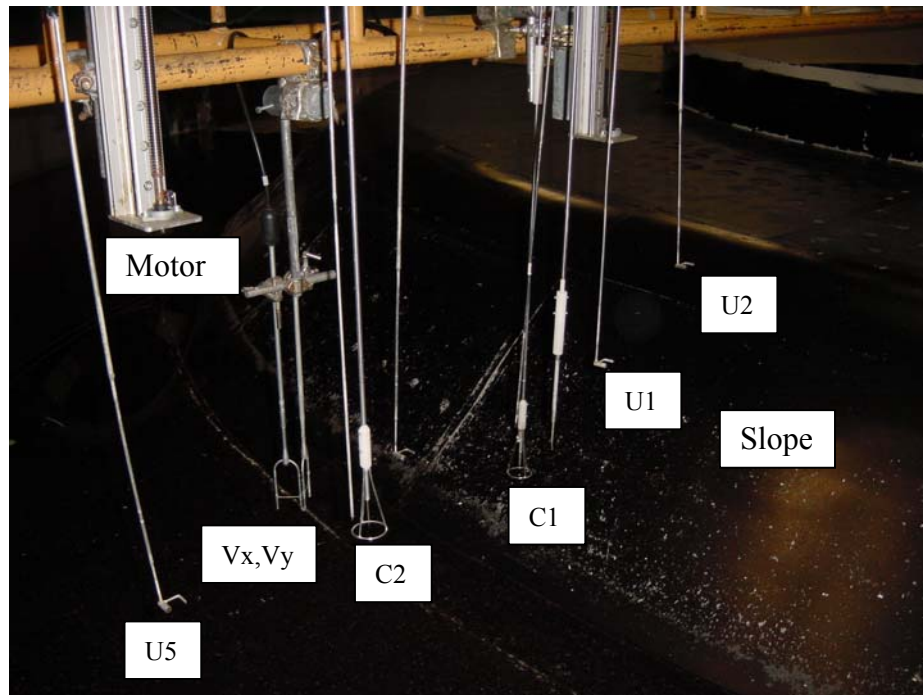
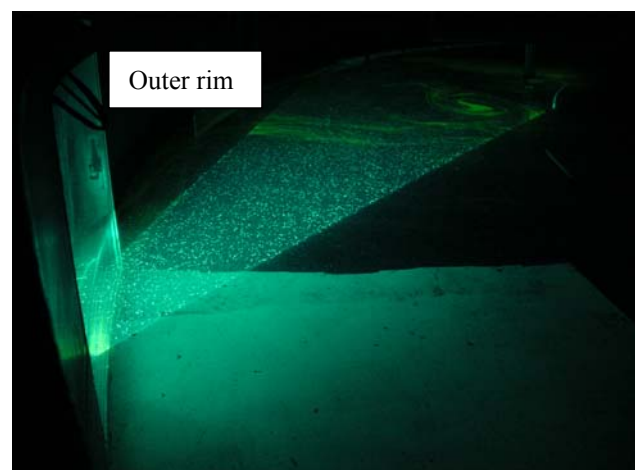


Figure 5: Photo of actual probe set-up. Ultrasonic (U) and conductivity (C) probes are discussed in text. Velocity probes give radial (V_x) and azimuthal (V_y) velocities.

Figure 6 Horizontal laser sheet employed for PIV measurements and fluorescein dye.



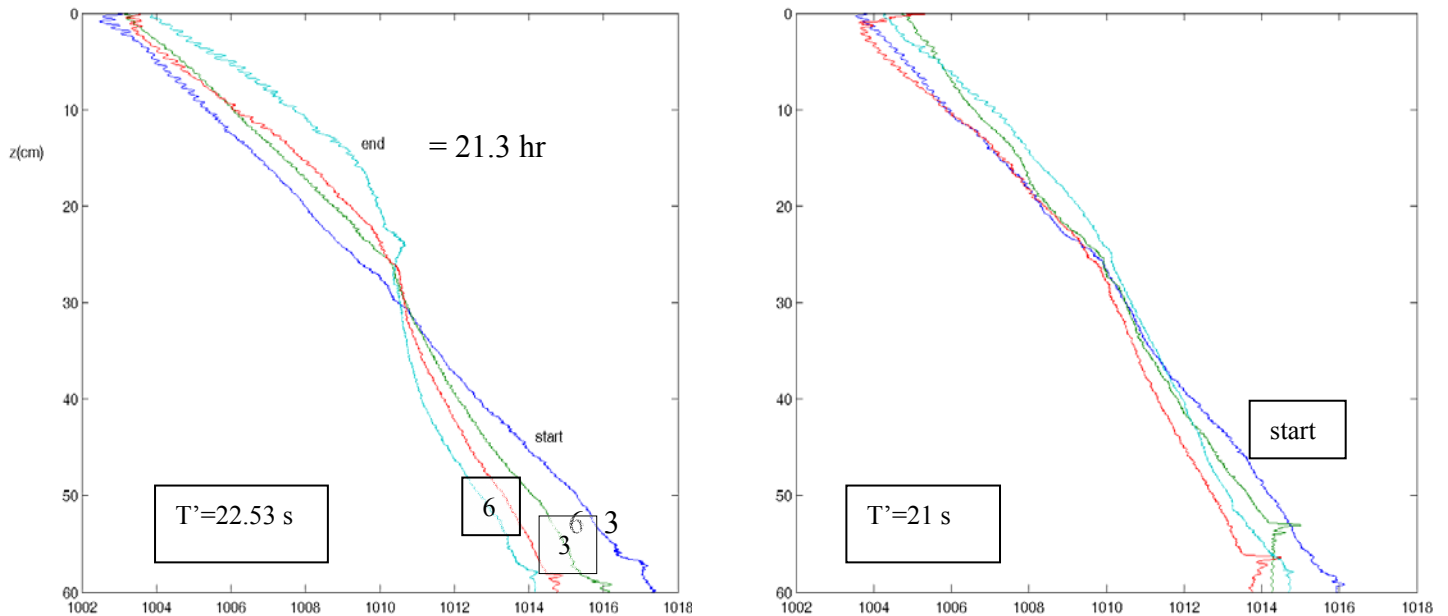


Figure 7 Observed density profiles for two different modulation periods T' during axisymmetric experiments. At start modulation is performed over a period of 1 hr. At left, another modulation of 1 hr duration is carried out after 3 hrs. At the right observations were at 1, 3 and 4.3 hrs after the start.

1.3 Results

3.1 Axisymmetric experiments

In a first trial experiment modulation was performed during $\tau=6$ hours, with $V=6$ cm/s, and a modulation period ($T'=22.53$ s) aimed at reaching the 1-1 attractor in the vertical-radial plane. At the end, the modulation was stopped, but the solid background rotation continued. Observations 64 hrs later showed that the stratification was “destroyed”. No explanation in terms of power failure was found. It was concluded that the mixing was produced by the oscillation. This experiment was repeated under milder conditions. The forcing amplitude being reduced to $V=3$ cm/s, lasting 1 hr only (see fig. 7). Fig. 8 shows the intensity of the radial velocity at a fixed azimuthal position (y), for varying radial positions (x) as a function of time. It demonstrates largest radial velocities near the sloping bottom (at the right) and propagation away from the slope. The response is clearly varying at the forcing period.

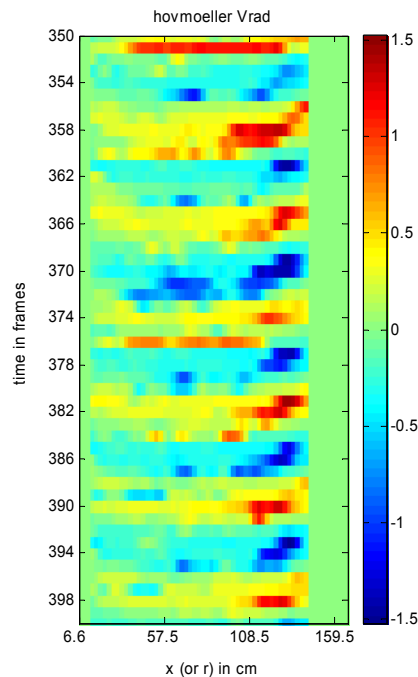


Figure 8: Radial velocity in time – space diagram. Inner slope is at the right.

3.2 Experiments with barrier

Inserting a radial barrier (Fig. 9) modulation of the rotation speed forces waves more directly, as in classical internal tide generation. Vertical laser sheets were analysed. It was found that the first two Empirical Orthogonal Functions reflect more the back and forth primary oscillatory motion in the azimuthal direction than the waves per se. This is because the laser sheet has a finite width (thus falsely projecting some of that motion into the radial and vertical direction), and because friction near the bottom yields a turning of the 'tidal' flow, leading to a genuine periodic motion in the plane of motion, unrelated to the internal waves. Empirical functions 3 and 4 (in Fig. 10 represented by the real and imaginary parts of the horizontal (u) and vertical (v) velocity components) seem to show rectilinear, sloping wave motion. This is in line with an expected oblique propagation of internal waves. Checks concerning the correspondence of observed angle with the angle predicted by the dispersion relation will be carried out.

Figure 9: Photo of movable barrier (radial black structure).

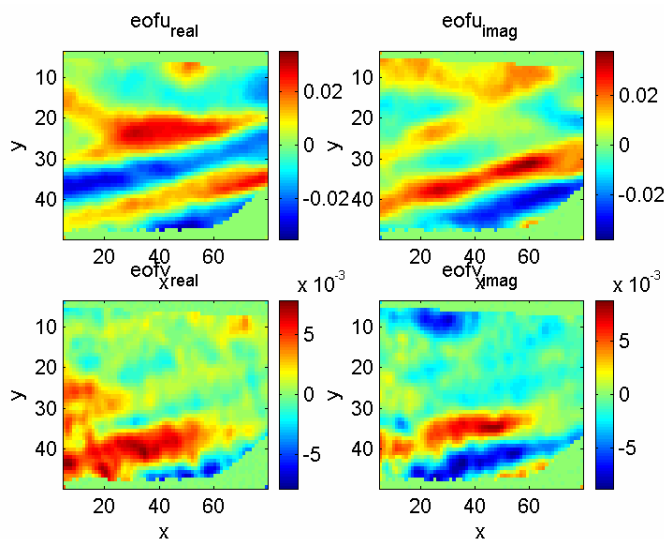
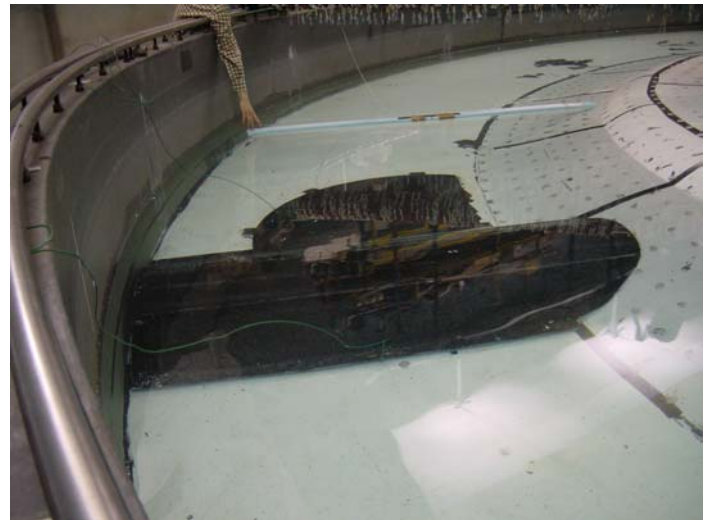


Figure 10: Vertical structure empirical Orthogonal functions 3&4 show Oblique wave propagation. Upper (radial velocity), lower panels (vertical velocity).

Simultaneous observations were carried out with the probes. The results in Fig. 11 present the observations of one day. This contains many angular positions of the barrier. Typically the barrier was inserted at a certain angular position (azimuth) and modulation was turned on for 5 minutes only (with a rim velocity $V=1$ cm/s only, as the forcing is much more efficient). Then observations were continued for another 25 min, after which it was assumed that the waves (here of 21 s period) had died out. The barrier was then moved slowly to a new position (this presents the white gaps in this figure), and the procedure started again. Density observations from 5 probes were followed and are listed in the lower five lines of each panel. The upper line gives radial velocity. Measurements were converted to density perturbations by using their calibration files. Typically what one can see is that the most intense waves are obviously present when the barrier is close to the probes. There is an indication that the waves while being more intense in the retrograde direction ('behind the barrier') they tend to propagate farther in the prograde direction. This will be studied closer by looking at blow-up and rescaled versions of this figure. This was in line with direct visual observations. What is not shown here is that there were vortices developing, possibly as a result of the mixing, although it may also have resulted from dragging the barrier from one to the next angular position.

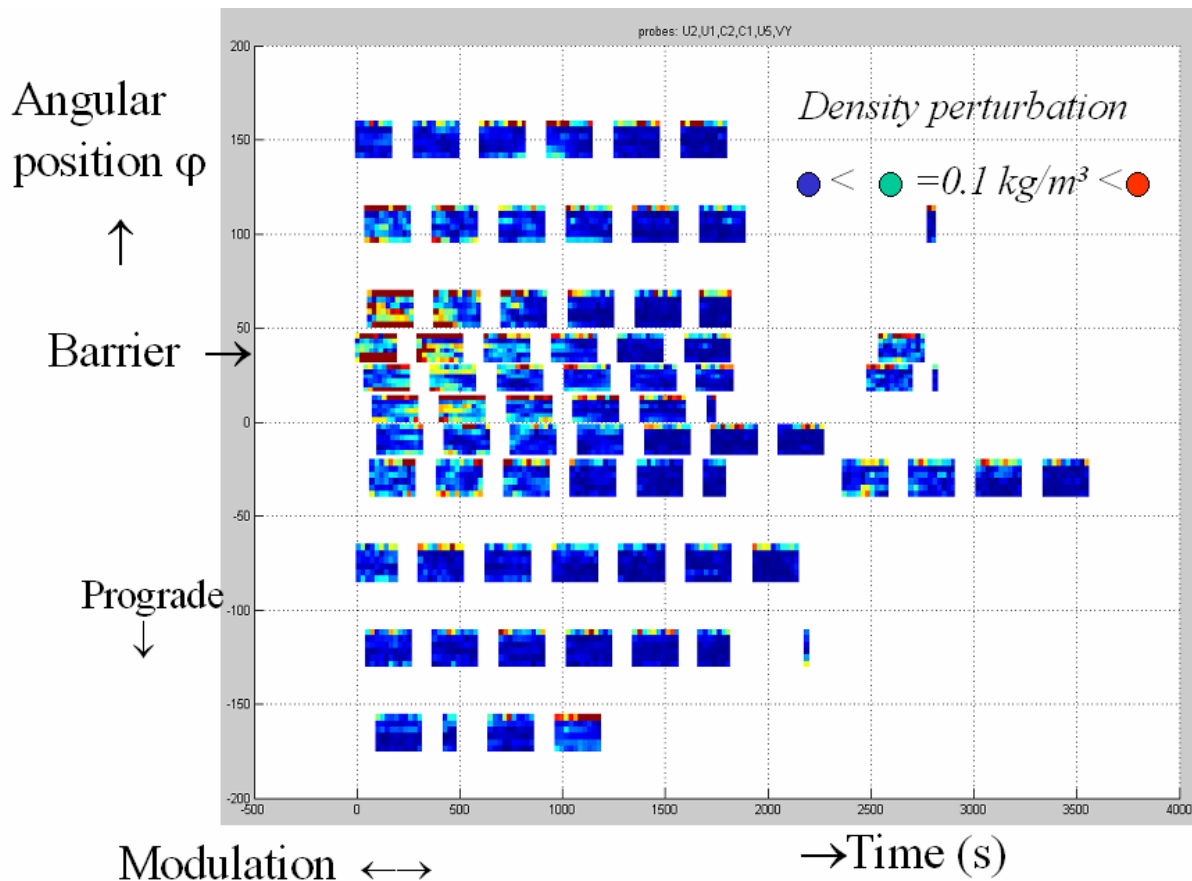


Figure 11. Results of probe measurements during experiments with barrier. Each panel consists of 6 lines giving, from the bottom upwards, 5 density probes and 1 radial velocity probes. The lowest line gives the innermost probe, U2, and then U1, C2, C1, U5. Each bin, within a line gives the amplitude of the density perturbation at modulation period estimated from a time interval lasting two such periods.

Time-space diagrams were also made from PIV observations just over the barrier (Fig. 12). The left diagram shows that during modulation (upper part of figure) radial velocity is uniform in strength with radial position. Only after stop of the wave forcing does an asymmetry develop, indicating waves now propagate also in the radial direction. This implies refraction may be operating. The diagram at the right, showing the radial velocity as a function of azimuthal distance, shows that the barrier is sending off waves in both prograde (right) and retrograde (left) direction. Once the modulation stops, an asymmetry develops showing the waves to last longer on the prograde side.

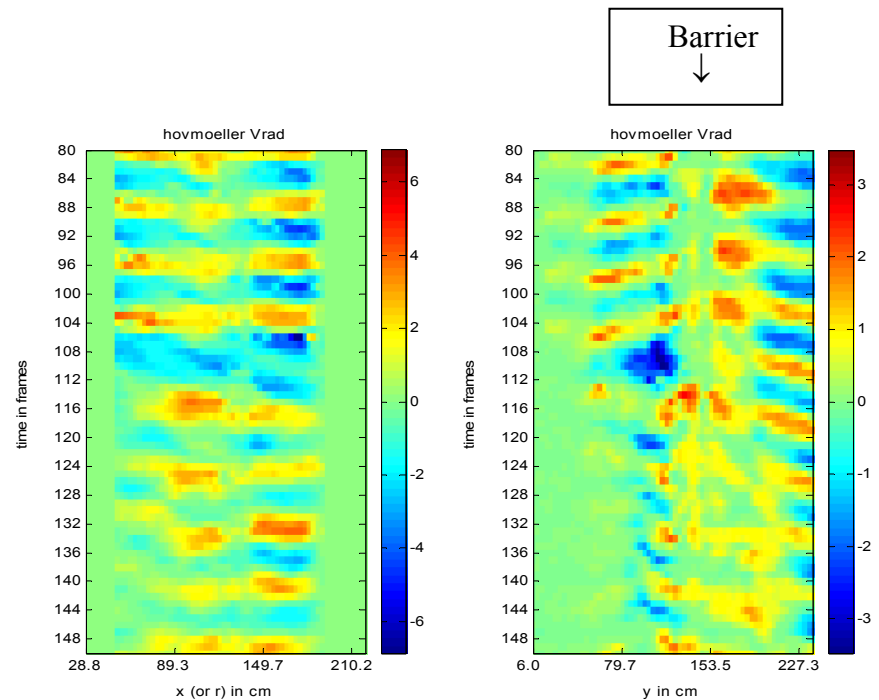


Figure 12: Time-space plot of radial velocity in radial (left) and azimuthal (right) direction. Barrier is at $y=153$ cm.

1.4 Conclusions

Experiments with modulation of rotation speed show in axisymmetric setting:

- enhanced mixing,
- internal waves propagating away from slope.

With radial barrier inserted waves are more easily generated, propagate in both directions, but show asymmetry in response, and some trapping near the barrier.

1.5 Acknowledgement

Help with data acquisition and processing by F.Eijgenraam, and the Coriolis team (S. Vibaud, H. Didelle, O. Praud, A. Fincham, S. Mercier, E. Thivolle and J. Sommeria) is gratefully acknowledged. The access to the experimental facility of the Coriolis Laboratory was supported by the European Commission, Enhancing Access to Research Infrastructures action of the Improving Human Potential programme of FP5, under contract HPRI-CT-1999-00006.

1.6 References

- Beardsley, R.C. (1970) An experimental study of inertial waves in a closed cone. *Stud. Appl. Math.* 49,187-196.
- Maas, L.R.M. (2001) Wave focusing and ensuing mean flow due to symmetry breaking in rotating fluids. *J. Fluid Mech.* 437, 13-28
- Maas, L.R.M. and Lam, F.-P. A. (1995) Geometric focusing of internal waves. *J. Fluid Mech.*, 300, 1-41
- Maas, L.R.M., D. Benielli, J. Sommeria and Lam, F.-P.A. (1997) Observation of an internal wave attractor. *Nature* 388, 557-561.
- Trowbridge J.H. and Lentz, S.J. (1991) Asymmetric behaviour of an oceanic boundary layer above a sloping bottom. *J. Phys. Oceanogr.* 21, 1171-1185.